Study of the upper energy limit of useful epithermal neutrons for Boron Neutron Capture Therapy in different tissues

Pablo Torres-Sánchez, Ignacio Porras, Fernando Arias de Saavedra, Javier Praena

Departamento de Física Atómica, Molecular y Nuclear, Facultad de Ciencias, Universidad de Granada, E-18071 Granada, Spain

Abstract

In Boron Neutron Capture Therapy (BNCT), the IAEA recommendations limit the epithermal range to 10 keV. Few works have shown the possibility to increase this limit. In particular, in a previous work we showed this possibility by means of simulations of the dose on a simple phantom of a 4-component ICRU tissue. This possible increment is very relevant for the future accelerator-based neutron sources for BNCT. The present work is based on more realistic MCNP6.2 simulations at neck, brain and abdomen. Several parameters and Figures of Merit have been evaluated for different beam apertures and beam divergences. The results show that neutrons above 10 keV can be useful for BNCT. The exact limit of the epithermal range depends on the location of the tumor.

Keywords: Boron Neutron Capture Therapy (BNCT), epithermal neutrons, accelerator-based BNCT, IAEA recommendations, Monte Carlo simulations

1. Introduction

Boron Neutron Capture Therapy (BNCT) is an experimental form of radiotherapy of increasing interest in recent years. Accelerator-based BNCT has prompted the development of a wide range of projects worldwide to bring this therapy closer to the hospitals. In the design of neutron beams for BNCT, certain restrictions to beam quality apply. This is the case of the definition of epithermal neutrons up to 10 keV, and thus the extent of the contribution of fast neutrons to the dose. The IAEA established some recommendations (IAEA, 2001), defined in the scope of reactor-based BNCT, for the desired neutron beam for deep seated tumors. These restrict the contribution of gamma radiation and fast neutrons to the beam respect to the flux of epithermal neutrons, defined as those with energies between 0.5 eV and 10 keV, as a commonly used criterion with no further arguments. The constraint for the fast neutron contribution to the beam was intended to reduce the production of high LET protons, which comes from the high energy tail of the spectrum from a reactor, that usually extends to a few MeV. However, the energy spectra of the new accelerator-based neutron beam differ from those of reactors, i.e. high LET protons can be somewhat avoided. Therefore, the epithermal limit should be revised taken into account the particularities of the accelerator-based neutron sources, as the cyclotron-based system in Kyoto (Tanaka et al., 2011).

Different researchers have studied the optimal neutron energy for epithermal beams in BNCT, finding it around 10 keV (Bisceglie et al., 1999) down to 2 keV (Nievaart et al., 2004). These studies used brain models and asserted that skin and bone thickness strongly influence this result. Indeed, these have showed that the IAEA definition comes close to the optimal neutron energy, and hence some suggested that a shift might be needed, rising it up to 50 keV (Bisceglie et al., 1999), while others claim that it should not be increased and be maintained at 10 keV (Seki et al., 2017). There are other proposals that include different approaches, with a different level of suppression for neutrons from 10 to 100 keV, and those above 100 keV, which must be strongly suppressed (Rasouli and Masoudi, 2015).

Accordingly, the actual value of the limit restricts the design and configuration of Beam Shaping Assemblies (BSA) in order to make the neutron beam suitable for treatments. Some authors have chosen not to use the epithermal-fast limit and rely only on the in-phantom Figures of Merit (Allen and Beynon, 2000). Another option is to shift this limit for their design by moving it to a higher energy, such as 40 keV (Tanaka et al., 2011; Faghihi and Khalili, 2013). Most of these works have tested the dosimetry using brain models. Others have followed the traditional definition at 10 keV, and analyzed the performance of their BSA using different target tumors in various body regions (Herrera et al., 2013).

In a paper of Yanch and Harling (Yanch and Harling, 1993) a thorough study of the dependence on the Figures of Merit on the neutron energy showed that energies above 10 keV are effective for BNCT. Also, in a previous article from the authors of this paper, it was analyzed the epithermal limit in a simple tissue model (Torres-Sánchez et al.,

*Corresponding author
Email address: porras@ugr.es (Ignacio Porras)

2019). However, as this limit depends on the tissue and the geometry of the body region, we present in this work a more detailed study by using three different more realistic phantoms of different body regions which differ on tissue compositions and represent main targets of BNCT. Also, different boron concentrations (in tumor and normal tissue) are taken into account in the present study which extends the results of the previous paper above-mentioned.

This paper is structured as follows. In Section 2, we describe the simulations that were carried out and the input data used. Section 3 discusses the results from these simulations and focuses on the pertinent figures. Finally, the conclusions derived from this research are highlighted in Section 4.

2. Materials and Methods

The dose deposition produced by neutron interaction was evaluated for several tissues by using Monte Carlo simulations. The MCNP6.2 code (Werner et al., 2018), was used to perform the simulations. The body regions analyzed were the brain, head and neck, and the liver at the abdomen. The Snyder model was used for skull and brain. The MIRD-ORNL male model was used for the neck and the abdomen (Goorley, 2008). Dose was calculated using F4 tallies, weighted by their corresponding kerma factors, computed following Goorley et al. (2002). The total dose in the tissue (D) was computed as the sum of the contributions to the dose by thermal neutrons (D_t), fast neutrons (D_f), boron (D_B) and gamma radiation (D_γ), weighted by their respective RBE factors (w_i), following:

$$D = w_t D_t + w_f D_f + w_B D_B + w_\gamma D_\gamma \quad (1)$$

where the RBE and boron concentration assumed were those shown in Table 1:

	w_t	w_f	w_γ	w_B	$[B]$ (ppm)
Normal	3.2	3.2	1	1.3	10, 25
Tumor				3.8	25-40, 62.5-100

Table 1: RBE factors and boron concentrations (for normal tissue and tumor) that have been used in the estimations of the total dose.

The simulations were carried out with monoenergetic, parallel and homogeneous neutron beams of two diameters (10 and 25 cm) onto the body regions of interest. Additionally, some simulations were made with changes in the beam divergence. In these cases, a beam divergence (J/ϕ) of 0.7 was used. This was achieved by means of a uniform cosine distribution between 0.44 and 1.0. Apart from these, two realistic case examples are given. In the first one, a dose map of a slice of the Snyder brain model with a monoenergetic beam above the 10 keV limit is given. In the second one, a realistic beam with a spectrum inspired in that of CBENS, with an aperture diameter of 25 cm and (J/ϕ) of 0.7 is used. In the latter, different energy cutoffs were applied to the spectrum to show the effect of neutrons slightly above 10 keV in the degradation of the beam quality. In all cases, a discretization of the tissue along the beam axis was implemented in order to study the dose deposition produced by the neutrons. For the Snyder model, the standard discretization with voxels of 0,4 cm along the beam axis. For abdomen and neck in the MIRD-ORNL model, the voxel width was 0.5 cm. For the thermal neutron scattering on hydrogen, the treatment of scattering on hydrogen in light water at 300 K has been used instead of the free gas model. Different Figures of Merit (FoM) have been evaluated: (i) the Advantage Depth (AD), as the maximum distance at which the dose in tumor exceeds the maximum dose in healthy tissue; (ii) the Double Dose Depth (DDD), as the maximum depth at which the dose in tumor is at least twice as much as the maximum dose in normal tissue; (iii) the Triple Dose Depth (TDD), as the maximum depth at which the dose in tumor is at least trice as much as the maximum dose in normal tissue and (iv) the Maximum Therapeutic Ratio (MTR), as the maximum tumor to normal tissue dose ratio. The behaviour of these FoM with respect to the neutron energy has been studied for the energy range between 1 keV to 50 keV.

3. Results and Discussion

In Figure 1 a color map of the ratio between the tumor dose and the maximum dose in normal tissue is displayed as a function of depth (X-axis) and initial neutron energy (Y-axis) for the example case of 10 cm diameter and boron concentrations of 10 ppm (normal tissue) and 35 ppm (tumor). The advantage depth (AD) corresponds to the depth at which the color changes from green to blue, and the double dose depth (DDD) to where the color changes from yellow to green. The triple dose depth (TDD) corresponds to the change of color from orange to red.

Our results show variability when considering the body region. The tumor dose is higher than twice the maximum at healthy tissue (i.e. the DDD exists) up to 15 keV for the neck, 23 keV for the brain and 25 keV for the abdomen. The TDD exists up to 7 keV (neck), 13 keV (brain) and 14 keV (abdomen), Figure 1 provides clear and compact illustrations of the results from the simulations. The AD reduces as the neutron energy increases and the area of full applicability of BNCT ceases to exist in 15-25 keV depending on the body region. In addition, for all cases, the simulations confirm that the optimum energy for BNCT treatments is around 1-7 keV, where the maximum dose ratio is achieved, and also the AD reaches more depth.

Considering each body region, comparisons can be extracted. For the neck, due to its smaller size, thermal and boron doses are less intense as a greater amount of neutrons fall outside the body before the complete thermalization, thus giving a higher relative relevance to the fast neutron component due to elastic collisions and hydrogen recoils. This makes the limit lower in energy when compared to brain or the abdomen. In the same direction, the

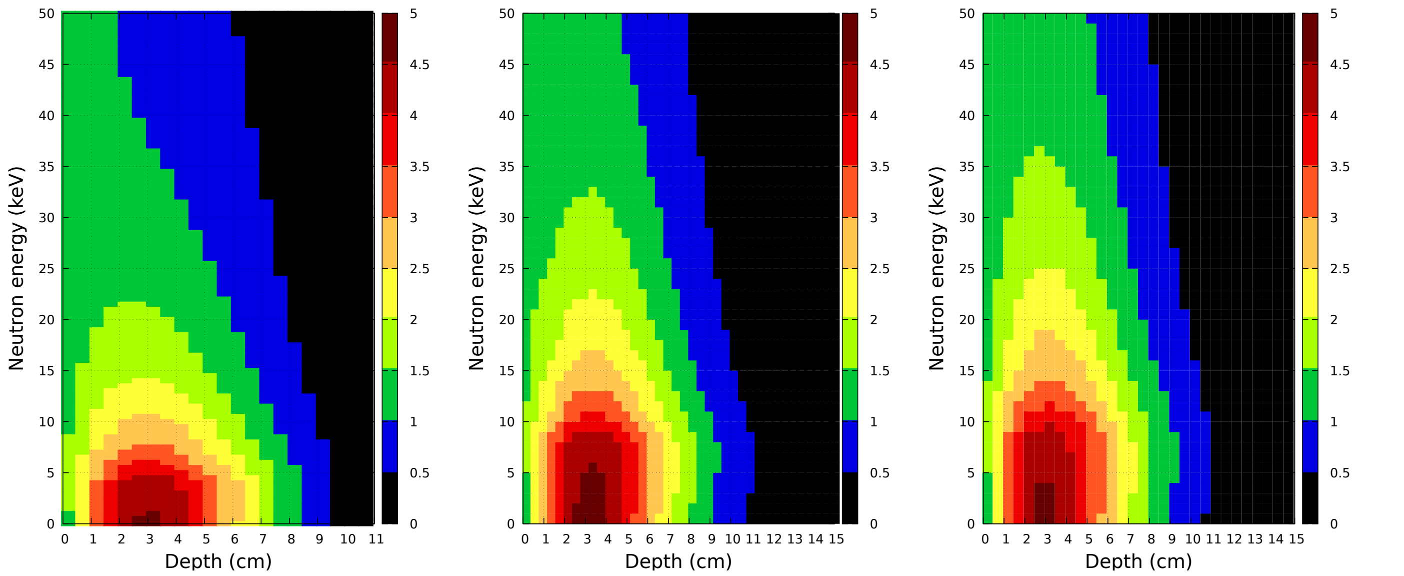

Figure 1: Ratio between the tumor dose and the maximum dose in normal tissue (color) as a function of depth (horizontal axis) and of the neutron energy (vertical axis). The figure on the left corresponds to the neck, the center to the brain and the right to the abdomen. The color scale has been chosen such that transitions from blue to green, green to yellow and orange to red show the position of the AD, the DDD and the TDD, respectively.

thermalization is more complete at the abdomen where a greater bulk of mass is present.

For other values of the irradiation parameters considered in this work (beam aperture and boron concentrations) the figures are similar but the values of Figures of Merit vary. In Table 2 we show the results obtained for the following quantities: maximum advantage depth (AD_{Max}), range of neutron energies for which the maximum AD is found ($E(AD_{Max}$ range), maximum double dose depth (DDD_{Max}), maximum energy for which the DDD exist ($E_{Max}(DDD)$), maximum triple dose depth (TDD_{Max}), maximum energy for which the TDD exists ($E_{Max}(TDD)$), the maximum value between all energies for the maximum therapeutic ratio (MTR_{Max}) and the neutron energy for which the maximum of MTR is found ($E(MTR_{Max})$). T/N denotes the ratio of boron concentration between tumor and normal tissue.

From the values of Table 2, it can be clearly seen how the upper energy limit of useful neutrons increases with the beam aperture, the boron concentration for a given T/N ratio, and with the T/N ratio for a given boron concentration in normal tissue. For example, for the beam aperture of 25 cm diameter, with the same boron concentrations used in Figure 1, the TDD exists up to 23 keV in neck, 34 keV in brain and more than 50 keV in the abdomen, and the TDD exists up to 12, 20 and 24 keV, respectively. If the boron concentration increases from 10 to 25 ppm in normal tissue (for the same T/N ratio of 3.5), these values for the TDD increases highly, to 36 keV for the neck and more than 50 keV for the other phantoms. As expected, an increase of the T/N ratio for the same rest of parameters produce an increase in the energy limiting values for DDD and TDD.

The maximum therapeutic ratio also increases rapidly with the boron concentration and T/N ratio, but decreases slightly for the larger aperture. It is worth to point out that the energy for which the maximum therapeutic ratio is found is always in a very short range (2-3 keV).

In Figure 2 we analyze the maximum therapeutic dose ratio (MTR) as a function of the initial neutron energy. From the observation of the plots a tendency change is evidenced for the different body regions. First, below a certain edge energy, the MTR is mostly flat. After that edge, the TR declines gradually becoming marginally higher than 1 near 50 keV (i.e. the maximum dose in the tumor is rather the same as in the normal tissue). This is due to the increasing relevance of the dose delivered by fast neutrons (before thermalized) in the total dose. For the small beam aperture (10 cm diameter), the energies for the position of this edge are 5 keV for the neck, 9 keV for the brain and 10 keV for the abdomen. However, for the case of the larger aperture (25 cm diameter), the energies for which MTR start decreasing are higher, clearly above 10 keV for the brain and abdomen.

Nevertheless, this tendency change does not imply the actual energy limit for the applicability of neutrons, since close beyond this edge the neutrons still show a desirable behavior, as they are able to produce higher dose at tumor than in normal tissue, so are still adequate for BNCT. Nonetheless, this advantage progressively reduces and ceases to be effective around 20-40 keV as previously stated. It seems that neutrons are still useful for BNCT at least up to 20-40 keV.

In Figure 3 we also illustrate, for the Snyder head phantom case, a 2-D dose map in a central cut of the brain for a monoenergetic beam of 15 keV neutrons. The colors

Boron Uptake (ppm)	T/N Ratio	Aperture Diameter (cm)	AD_{Max} (cm)	$E(AD_{Max})$ Range (keV)	DDD_{Max} (cm)	E_{Max}(DDD) (keV)	TDD_{Max} (cm)	E_{Max}(TDD) (keV)	MTR_{Max}	$E(MTR_{Max})$ (keV)
			Neck							
10	2.5	10	7.75	1-6	5.75	10	4.25	5	3.45	2
		25	7.75	1-10	5.75	15	3.75	6	3.2	2
	3	10	8.25	2-5	6.25	13	4.75	7	3.95	2
		25	8.25	1-9	6.25	19	4.75	9	3.7	2
	3.5	10	8.25	1-6	6.75	15	5.25	8	4.55	2
		25	8.75	4-7	6.75	23	5.25	12	4.2	2
	4	10	8.75	2-5	7.25	17	5.75	10	5.15	2
		25	8.75	1-9	7.25	27	5.75	14	4.75	2
25	2.5	10	8.25	1-12	6.75	26	5.75	15	4.8	2
		25	8.75	2-14	7.25	43	5.75	22	4.6	2
	3	10	8.75	1-11	7.25	33	6.25	19	5.75	2
		25	9.25	9-10	7.75	>50	6.25	29	5.45	2
	3.5	10	8.75	1-13	7.75	39	6.75	23	6.65	2
		25	9.25	2-15	7.75	>50	6.75	36	6.3	2
	4	10	9.25	2-10	7.75	47	6.75	27	7.55	2
		25	9.25	2-18	8.25	>50	7.25	43	7.15	2
			Brain							
10	2.5	10	8.6	2-10	7	16	4.6	9	3.5	2
		25	10.2	8-14	7.4	24	5	14	3.3	2
	3	10	9	4-9	7	19	5.4	11	4	2
		25	10.6	6-14	8.2	29	6.2	17	3.9	2
	3.5	10	9.4	6-8	7.4	23	5.8	13	4.65	2
		25	11	7-13	8.6	34	7	20	4.45	2
	4	10	9.4	2-10	7.8	26	6.2	16	5.25	2
		25	11.4	11-13	9	40	7.4	23	4.95	2
25	2.5	10	9.4	4-16	7.4	41	6.2	24	4.9	3
		25	11.4	20-21	9	>50	7.4	37	4.75	2
	3	10	9.8	4-16	8.2	>50	7	30	5.8	3
		25	11.8	16-21	9.4	>50	8	47	5.65	2
	3.5	10	10.2	6-16	8.6	>50	7.4	35	6.75	2
		25	12.2	19-20	9.8	>50	8.6	>50	6.45	2
	4	10	10.6	7-15	9	>50	7.8	42	7.65	2
		25	12.2	6-26	10.2	>50	9	>50	7.4	2
			Abdomen							
10	2.5	10	8.25	1-11	6.25	18	4.25	10	3.45	2
		25	9.75	11-15	6.75	30	4.25	9	3.15	3
	3	10	8.75	2-10	6.75	21	5.25	12	4	3
		25	10.25	12-15	7.25	36	5.25	19	3.6	3
	3.5	10	9.25	5-9	7.25	25	5.75	14	4.55	3
		25	10.25	5-19	7.75	43	5.75	24	4.1	3
	4	10	9.25	2-11	7.25	29	6.25	17	5.15	2
		25	10.75	9-18	8.25	>50	6.75	29	4.6	3
25	2.5	10	9.25	4-18	7.25	46	5.75	26	4.8	3
		25	10.75	11-28	8.25	>50	6.75	45	4.55	3
	3	10	9.75	5-18	7.75	>50	6.75	33	5.75	2
		25	11.25	11-30	8.75	>50	7.25	>50	5.3	3
	3.5	10	10.25	8-16	8.25	>50	6.75	39	6.65	2
		25	11.75	17-30	9.25	>50	7.75	>50	6.2	3
	4	10	10.25	3-19	9.75	>50	7.25	47	7.55	2
		25	11.75	5-36	9.75	>50	8.25	>50	6.95	3

Table 2: Relevant FOMs extracted from the simulations are given. Data for Neck, Brain and Abdomen is given, considering boron concentrations in normal tissue of 10 and 25 ppm, and T/N ratios from 2.5 to 4.0. Two beam apertures (10 and 25 cm diameter) for the monodirectional beam are included.

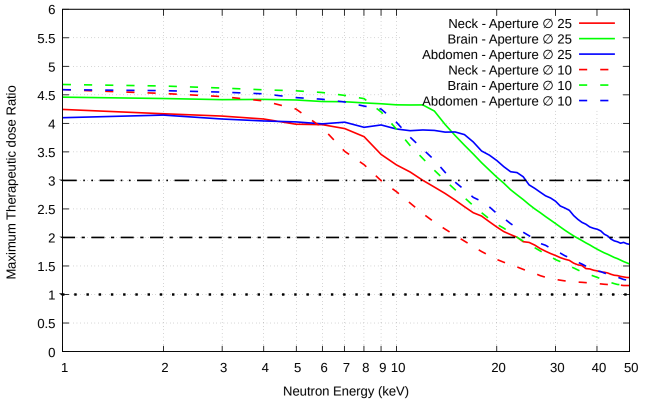

Figure 2: MTR as a function of the neutron energy for the three body regions studied. The cases with t/n ratio of 3.5 and low boron uptake (10 ppm) are shown. The reference values of MTR = 1, 2 and 3 are highlighted with the horizontal dotted, dotted-dashed and double-dotted-dashed lines, respectively. A change in the beam aperture can increase the suitability of higher energy neutrons, at a cost of lower TRs.

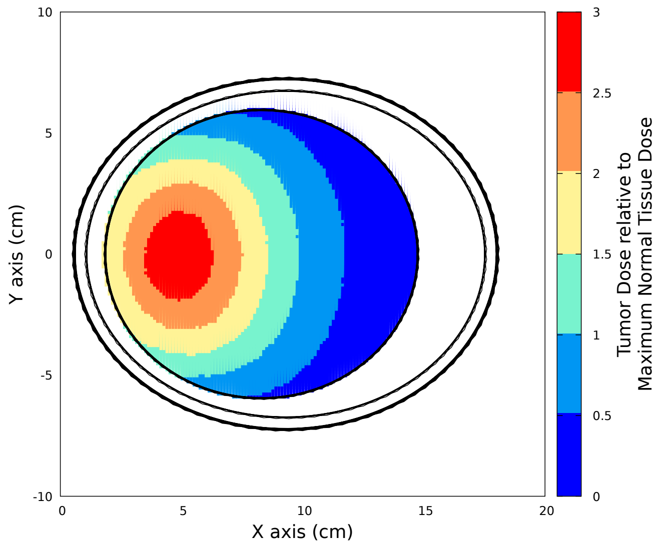

Figure 3: Ratio of the tumor dose and the maximum normal tissue dose in a central cut of a Snyder head phantom for monoenergetic neutrons of 15 keV.

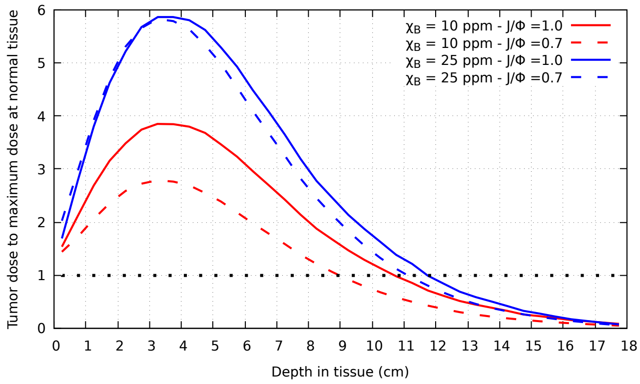

Figure 4: Tumor dose profiles relative to maximum dose at normal tissue in the Abdomen configuration, showing the differences arisen from different beam divergences. A neutron beam of monoenergetic 15 keV neutrons and a T/N ratio of 3.5 are fixed. The relevance of the beam divergence is revealed to be more relevant in patients with lower boron uptake.

represent the ratio between the tumor dose and the maximum dose in normal tissue at the different regions of the brain. There is a significant region in which the tumor dose exceeds the maximum normal tissue dose.

All the previous discussion has been done with monodirectional neutron beams of different energies. This is not fully realistic, as the beams that are obtained from accelerators will necessary have some beam divergence. For studying the effect of this divergence in the previous results we have simulated, for a neutron energy of 15 keV, a beam of neutrons with different directions ($J/\phi = 0.7$), which corresponds to the maximum divergence allowed in the IAEA recommendations). The comparison to the results for the monodirectional beam ($J/\phi = 1.0$) is illustrated in Figure 4 for the case of 25 cm diameter and T/N ratio of 3.5, for the two boron concentrations in normal tissue. It is worth to point out how the effect of the divergence is quite small for the case of the larger boron concentration but stronger (decreasing the quality of the dose profile) in the case of the smaller boron concentration. However, as it can be seen in the figure, 15 keV neutrons seem to be useful for BNCT, even if the beam has some divergence.

The present study has been focused on the range of energies appropriate for BNCT and a comparison between them, and for this reason monoenergetic beams of different energies are compared. However a realistic beam will have a continuous distribution of different energies. Therefore we have made a simplistic test on the impact on the suppression of the neutron tail from a different threshold energy, in order to determine which energy range are more responsible of a profile degradation. For this purpose we have simulated an idealistic neutron spectrum, inspired in the one of C-BENS (Tanaka et al., 2011) with four different cutoffs: neutrons up to 10 keV, neutrons up to 20 keV, neutrons up to 40 keV, and full spectrum. The depth dose profile in tumor (normalized to the maximum dose in normal tissue) is shown in Figure 5, for the case of 25 cm diameter, T/N = 3.5, 10 ppm of boron in normal tissue and divergence (J/ϕ) of 0.7. It can be noticed how the inclusion of the neutrons between 10 and 40 keV do not produce a significant effect on the depth dose profile, and that the inclusion of the high energy tail (beyond 40 keV) decreases significantly the maximum tumor dose and slightly the advantage depth.

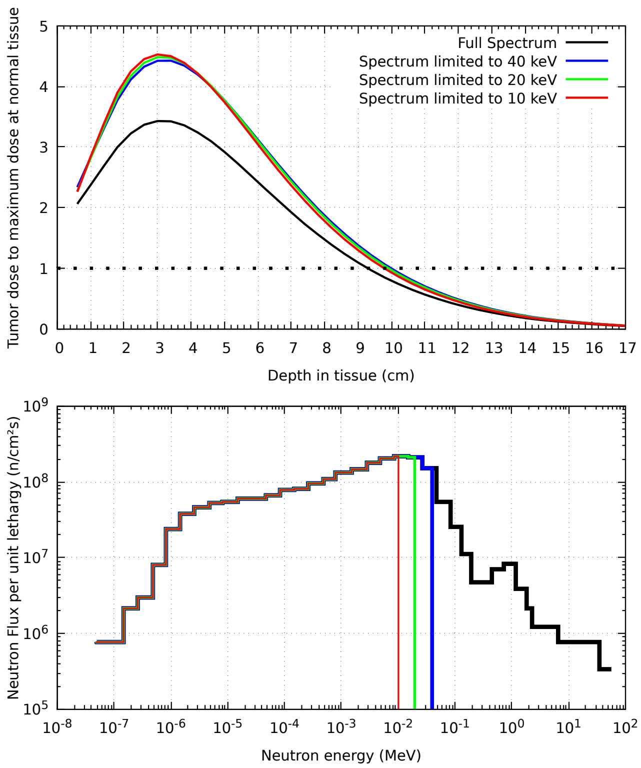

Figure 5: An example of the effect of the higher energy neutrons in a realistic beam with a divergence of J/ϕ of 0.7. A CBENS-like spectrum has been used, as shown in the lower panel. The different dose profiles in the upper panel correspond to the spectra shown below, which are related to a full spectrum, and some versions of it with a sharp limit at 40, 20 and 10 keV. The close matching among the limited-spectrum dose profiles, together with the clear difference when compared to the full spectrum one do manifest that the lower-than-40 keV neutrons are not a cause of the profile degradation.

4. Conclusions

The calculations here performed have confirmed, for more realistic phantoms, the results of the previous paper (Torres-Sánchez et al., 2019): there is a few keV range above the historically epithermal upper bound (10 keV) in which neutrons can be still useful for BNCT, since for those neutrons there exists a region in which the tumor tumor dose exceeds at least twice or trice the maximum dose in normal tissue. This region, previously determined up to 17 keV for a cylindrical phantom of 4-component ICRU tissue, can be extended to an energy spanning around 10 to 40 keV when assessing different body regions (as the brain, neck and abdomen studied here), boron concentrations and beam features as the aperture diameter. This suggests that the epithermal limit could be raised, at least to a conservative value of 20 keV.

In addition to this, the best neutron energy for BNCT of deep seated tumors, understood as the value for which the AD is maximum, was found to be in the range 1-30 keV and most commonly centered around 10 keV for the different cases studied. The neutron energy optimizing the MTR has been found to be consistently around 2-3 keV, while maintaining a similar value up to around 10 keV.

The results add some information to the current debate that establishing fixed criteria for the limit of the epithermal range do not necessary help in finding the best possible beam design. Here we show that there are useful neutrons above 10 keV and that the upper limit for obtaining a therapeutic effect is not the same for different phantoms, also considering the possible variability in boron uptake and T/N ratios, and beam physical features as its divergence or aperture diameter. Hence, the use of a fixed value for it (the upper energy limit) as the current recommendations may suggest, should be relaxed or at least raised to a slightly greater value (at least 20 keV).

The spirit of the upper limit of the energy of 10 keV in the IAEA-TECDOC-1223 (IAEA, 2001) is just an easily understandable value to delimit the energy range. The own document opens the possibility of using other limits, if they are clearly reported. In this sense we add more evidence to previous works. For example, from the results of Yanch et al. (1991), a limit for useful neutrons in the work of Tanaka et al. (2009) was set to 40 keV.

The present research highlights the importance of in-phantom evaluation for the design of a neutron beam for BNCT. This paper has studied the role of the different neutron energies, but of course real beams will have a continuous energy distribution. In order to achieve a criterion for the determination of the limit in each treatment the in-phantom Figures of Merit should be taken into account. When designing a neutron beam for BNCT, a reduction of the fast dose due to non-epithermal neutron by larger moderators also reduces the beam intensity, so all these considerations have to be balanced. In particular, we have determined that a neutron beam component slightly above 10 keV can be still useful for BNCT. Our results contribute to the set of studies on the epithermal limit for future discussions on the framework of the BNCT community.

Acknowledgements

We acknowledge financial support for this work from the Asociación Española Contra el Cáncer (AECC) under contract PS16163811PORR, Junta de Andalucía (Andalusian Regional Government), under contracts P11-FQM-8229 and A-FQM-371-UGR18 (FEDER Andalucìa 2014-2020 funds), the spanish MINECO and FEDER funds under contract FIS2015-69941-C2-1-P, and the donors of the University of Granada Chair Neutrons for Medicine: *Fundación ACS, Capitán Antonio, La Kuadrilla de Iznalloz* and *Sonriendo se Puede Ganar*. P.T. acknowledges a grant under the program Becas de Iniciación a la Investigación para estudiantes de Máster from the Universidad de Granada (Plan Propio de Investigación) and support from the Spanish Ministry of Science, Innovation and Universities under the FPU grant FPU17/02305.

References

References

Allen, D.A., Beynon, T.D., 2000. What is the best proton energy for accelerator-based bnct using the reaction? Medical Physics 27, 1113–1118. URL: https://aapm.onlinelibrary.wiley.com/doi/abs/10.1118/1.598976, doi:10.1118/1.598976.

Bisceglie, E., Colangelo, P., Colonna, N., Santorelli, P., Variale, V., 1999. On the optimal energy of epithermal neutron beams for bnct. Physics in Medicine and Biology 45, 49 – 58. URL: https://doi.org/10.1088/0031-9155/45/1/304, doi:10.1088/0031-9155/45/1/304.

Faghihi, F., Khalili, S., 2013. Beam shaping assembly of a d–t neutron source for bnct and its dosimetry simulation in deeply-seated tumor. Radiation Physics and Chemistry 89, 1 – 13. URL: https://doi.org/10.1016/j.radphyschem.2013.02.003, doi:10.1016/j.radphyschem.2013.02.003.

Goorley, J.T., Kiger III, W.S., Zamenhof, R.G., 2002. Reference dosimetry calculations for neutron capture therapy with comparison of analytical and voxel models. Medical Physics 29, 145–156. URL: https://aapm.onlinelibrary.wiley.com/doi/abs/10.1118/1.1428758, doi:https://doi.org/10.1118/1.1428758, arXiv:https://aapm.onlinelibrary.wiley.com/doi/pdf/10.1118/1.1428758.

Goorley, T., 2008. MCNP Medical Physics Geometry Database. Technical Report. URL: https://laws.lanl.gov/vhosts/mcnp.lanl.gov/pdf_files/la-ur-08-2468.pdf.

Herrera, M., González, S., Minsky, D., Kreiner, A., 2013. Evaluation of performance of an accelerator-based bnct facility for the treatment of different tumor targets. Physica Medica 29, 436 – 446. URL: https://doi.org/10.1016/j.ejmp.2013.01.006, doi:10.1016/j.ejmp.2013.01.006.

IAEA, 2001. Current Status of Neutron Capture Therapy. Number 1223 in TECDOC Series, International Atomic Energy Agency, Vienna. URL: https://www.iaea.org/publications/6168/current-status-of-neutron-capture-therapy.

Nievaart, V.A., Moss, R.L., Kloosterman, J.L., van der Hagen, T.H.J.J., van Dam, H., 2004. A parameter study to determine the optimal source neutron energy in boron neutron capture therapy of brain tumours. Physics in Medicine and Biology 49, 4277–4292. URL: https://doi.org/10.1088/0031-9155/49/18/006, doi:10.1088/0031-9155/49/18/006.

Rasouli, F.S., Masoudi, S.F., 2015. A study on the optimum fast neutron flux for boron neutron capture therapy of deep-seated tumors. Applied Radiation and Isotopes 96, 45 – 51. URL: https://doi.org/10.1016/j.apradiso.2014.11.016, doi:10.1016/j.apradiso.2014.11.016.

Seki, R., Wakisaka, Y., Morimoto, N., Takashina, M., Koizumi, M., Toki, H., Fukuda, M., 2017. Physics of epi-thermal boron neutron capture therapy (epi-thermal bnct). Radiological Physics and Technology , 387 – 408URL: https://doi.org/10.1007/s12194-017-0430-5, doi:10.1007/s12194-017-0430-5.

Tanaka, H., Sakurai, Y., Suzuki, M., Masunaga, S., Kinashi, Y., Kashino, G., Liu, Y., Mitsumoto, T., Yajima, S., Tsutsui, H., Maruhashi, A., Ono, K., 2009. Characteristics comparison between a cyclotron-based neutron source and kur-hwnif for boron neutron capture therapy. Nuclear Instruments and Methods in Physics Research Section B: Beam Interactions with Materials and Atoms 267, 1970 – 1977. URL: http://www.sciencedirect.com/science/article/pii/S0168583X09004224, doi:https://doi.org/10.1016/j.nimb.2009.03.095.

Tanaka, H., Sakurai, Y., Suzuki, M., Masunaga, S., Mitsumoto, T., Fujita, K., Kashino, G., Kinashi, Y., Liu, Y., Takada, M., Ono, K., Maruhashi, A., 2011. Experimental verification of beam characteristics for cyclotron-based epithermal neutron source (c-bens). Applied Radiation and Isotopes 69, 1642 – 1645. doi:https://doi.org/10.1016/j.apradiso.2011.03.020. special Issue: 14th International Conference on Neutron Capture Therapy.

Torres-Sánchez, P., Porras, I., de Saavedra, F.A., Sabariego, M., Praena, J., 2019. On the upper limit for the energy of epithermal neutrons for boron neutron capture therapy. Radiation Physics and Chemistry 156, 240 – 244. doi:https://doi.org/10.1016/j.radphyschem.2018.11.015.

Werner, C.J., Bull, J.S., Solomon, C.J., Brown, F.B., McKinney, G.W., Rising, M.E., Dixon, D.A., Martz, R.L., Hughes, H.G., Cox, L.J., Zukaitis, A.J., Armstrong, J.C., Forster, R.A., Casswell, L., 2018. MCNP6.2 Release Notes - report LA-UR-18-20808. Los Alamos National Laboratory (LANL).

Yanch, J.C., Harling, O.K., 1993. Dosimetric Effects of Beam Size and Collimation of Epithermal Neutrons for Boron Neutron Capture Therapy. Radiation Research 135, 131–145. URL: https://doi.org/10.2307/3578288, doi:10.2307/3578288.

Yanch, J.C., Zhou, X.L., Brownell, G.L., 1991. A monte carlo investigation of the dosimetric properties of monoenergetic neutron beams for neutron capture therapy. Radiation Research 126, 1–20. URL: http://www.jstor.org/stable/3578165, doi:https://doi.org/10.2307/3578165.